

Current Biology

Transcriptional Memory in the *Drosophila* Embryo

Highlights

- A live imaging technique reveals transcriptional memory in *Drosophila* embryos
- Memory nuclei exhibit higher probabilities of rapid post-mitotic reactivation
- Memory nuclei activate transcription twice as fast as inactive mothers

Authors

Teresa Ferraro, Emilia Esposito,
Laure Mancini, ...,
Aleksandra M. Walczak,
Michael Levine, Mounia Lagha

Correspondence

msl2@princeton.edu (M.L.),
mounia.lagha@igmm.cnrs.fr (M.L.)

In Brief

Ferraro et al. provide the first evidence of transcriptional memory in a multicellular organism. By monitoring the expression of stochastically expressed transgenes in living *Drosophila* embryos, Ferraro et al., visualize and quantify the extent to which transcription is inherited from mother to daughter cells in a living embryo.

Transcriptional Memory in the *Drosophila* Embryo

Teresa Ferraro,^{1,2,3,4} Emilia Esposito,^{5,6} Laure Mancini,⁵ Sam Ng,⁵ Tanguy Lucas,^{1,2,3} Mathieu Coppey,^{1,2,3} Nathalie Dostatni,^{1,2,3} Aleksandra M. Walczak,^{2,4} Michael Levine,^{5,6,*} and Mounia Lagha^{5,7,*}

¹Institut Curie, PSL Research University, UMR 3664/UMR 168, Paris 75248, France

²CNRS, UMR 3664/UMR 168/UMR 8549/UMR 8550, Paris 75248, France

³Sorbonne Universités, UPMC University Paris 06, UMR 3664/UMR 168, Paris 75248, France

⁴PSL, Ecole Normale Supérieure, UMR 8549, Paris 75005, France

⁵Molecular and Cellular Biology Department, GDD, University of California, Berkeley, Berkeley, CA 94720, USA

⁶Lewis-Sigler Institute, Department of Molecular Biology, Princeton University, Princeton, NJ 08544, USA

⁷IGMM, CNRS, UMR 5535, Montpellier 34293, France

*Correspondence: mnl2@princeton.edu (M.L.), mounia.lagha@igmm.cnrs.fr (M.L.)

<http://dx.doi.org/10.1016/j.cub.2015.11.058>

SUMMARY

Transmission of active transcriptional states from mother to daughter cells has the potential to foster precision in the gene expression programs underlying development. Such transcriptional memory has been specifically proposed to promote rapid reactivation of complex gene expression profiles after successive mitoses in *Drosophila* development [1]. By monitoring transcription in living *Drosophila* embryos, we provide the first evidence for transcriptional memory in animal development. We specifically monitored the activities of stochastically expressed transgenes in order to distinguish active and inactive mother cells and the behaviors of their daughter nuclei after mitosis. Quantitative analyses reveal that there is a 4-fold higher probability for rapid reactivation after mitosis when the mother experienced transcription. Moreover, memory nuclei activate transcription twice as fast as neighboring inactive mothers, thus leading to augmented levels of gene expression. We propose that transcriptional memory is a mechanism of precision, which helps coordinate gene activity during embryogenesis.

RESULTS AND DISCUSSION

New methods for visualizing gene activity in living *Drosophila* embryos provide a unique opportunity to investigate the kinetics of post-mitotic reactivation during development. Is the transcriptional status of a gene (active or inactive) inherited across cell generations during embryogenesis?

To date, the extent to which transcriptional activity is inherited from mother to daughter cells, referred to as transcriptional memory, has been directly recorded only in Dictyostelium and cultured mammalian cells [2, 3]. In the latter, live imaging of inducible fluorescent Polymerase II (Pol II)- and MS2-reporter transgenes reveals that the kinetics of Pol II recruitment and production of transcripts after mitosis are accelerated 13-fold and 5-fold, respectively [3]. Thus, inheritance of transcriptional activity across a cell lineage increases the rate of transcription and

may impact various developmental processes. Persistent memory was also observed at the protein level [4]. Transcriptional inheritance is lost in chromatin mutants (for example, *Ash2* mutants [2]) and is therefore attributed to an epigenetic bookmarking process during mitosis.

Here, we visualize the activities of stochastically expressed transgenes in order to distinguish active and inactive mother cells and the behaviors of their daughter nuclei after mitosis. We reasoned that a variety of transcriptional mechanisms—paused RNA Pol II, enhancer priming, and shadow enhancers—ensure precise timing of transcription reactivation after mitosis [5]. In previous experiments, the transgenes analyzed were activated in a rapid and synchronous manner, and this precluded a rigorous comparison of expressing and non-expressing nuclei through mitosis, obscuring the detection of potential transcriptional memory processes during early mitotic cycles in the *Drosophila* embryo [6, 7].

We employed sensitized transgenes that produce patterns of sporadic expression in order to trace the behaviors of individual cell lineages. By comparing the timing of gene reactivation of daughters originating from expressing (called memory nuclei) and neighboring non-expressing (non-memory) nuclei, we obtained evidence for transcriptional memory.

We focused our analysis on the regulation of *snail* (*sna*), which encodes a zinc-finger transcription factor that is essential for epithelial-mesenchyme transitions (EMTs) in most animal systems [8]. It has been implicated in a variety of developmental and disease processes, including mesoderm invagination in *Drosophila* [9] and metastases of cancerous tissues [8]. In *Drosophila*, *sna* is expressed in a thousand cells comprising the embryonic mesoderm [10], where it is important for coordinating their invagination during gastrulation [9]. Paused Pol II helps to coordinate the activation of *snail* transcription in the different cells of the mesoderm [11], while “redundant” mesodermal enhancers provide robustness in the activation of *sna* expression, even under stressful conditions such as elevated temperatures [12, 13].

A 500 bp region of the distal *sna* (shadow) enhancer (*snaE*) was attached to a *yellow* reporter gene containing 24 MS2 stem loops (Figure 1A). This minimal enhancer lacks three Zelda binding sites [14, 15], which are likely to be important for the timely activation of the endogenous *sna* gene during early stages of development [16]. This truncated enhancer

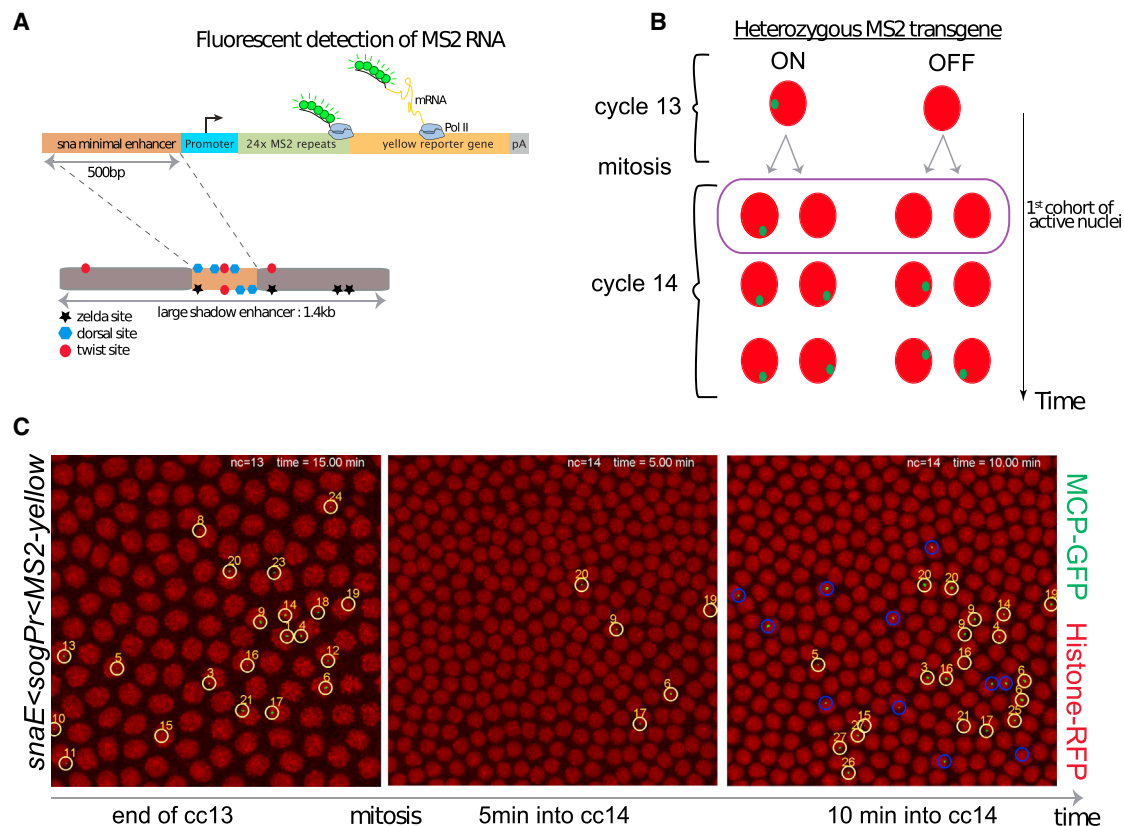


Figure 1. Live Imaging of a Sensitized *snail* Transgene Reveals Transcriptional Memory

(A) Schematic view of a sensitized *snail* transgene. A minimal 500 bp *snail* shadow enhancer was cloned upstream of various minimal promoters and 24X MS2 repeats, followed by a *yellow* reporter gene. Upon activation, the MS2 stem loops in nascent transcripts are bound by a MCP-GFP fusion protein.

(B) Schematic representation of transcriptional memory. Descendants from transcriptionally active mother nuclei in nuclear cycle 13 (cc13) tend to activate transcription very early during interphase 14, circled and referred to as “first cohort of active nuclei.” This particular population is referred to as “memory” nuclei, whereas active descendants from inactive mother nuclei at cc13 are referred to as “non-memory” nuclei.

(C) Live imaging of the transcriptional activity of a sensitized *snail* transgene (*snail-enhancer<sogPr<MS2-yellow*). Nascent mRNA “spots” are shown in green (MS2-MCP-GFP), and nuclei are labeled in red (histone-RFP transgene). Only selected time frames are shown; the entire movie can be obtained in [Movie S1](#). All active nuclei at cc13 were tracked with a unique number. After mitosis, their descendants (circled in yellow) were tracked; active cc14 nuclei derived from inactive mothers are circled in blue. Ventral views of a 2.1 × zoomed central region of an embryo, where anterior is to the left, are shown.

See also [Figure S1](#) and [Movie S1](#).

also lacks two Twist binding sites, which are known to act synergistically with Dorsal for the activation of *snail* expression [17]. The minimal enhancer was used in combination with several different core promoters, and each construct was integrated, as a single copy, in the same landing site using the PhiC31-integrase-mediated site-specific transgenesis method [18]. These minimal promoters include, e.g., *sna* and *brinker* (*brk*), which contain paused Pol II, and others, e.g., *wntD*, that lack it [11, 19]. All of the resulting *snaE<MS2-yellow* heterozygous transgenes exhibited slow expression dynamics (see [Movies S1](#) and [S2](#)). Activation was not clearly observed until nuclear cleavage cycle 13 (nc13), and only in a fraction of the nuclei (~10%–20%), whereas the endogenous locus is normally expressed in all nuclei of the presumptive mesoderm during this cycle ([Figures 1C](#) and [S1](#)).

Transcription is not detected during mitosis 13, but is reactivated during nc14. The kinetics of this activation is slow and stochastic among nuclei and does not encompass all of the nuclei comprising the mesoderm until after 30–40 min after mitosis ([Fig-](#)

[ures 1](#) and [S1](#); [Movie S1](#)). In contrast, the endogenous gene exhibits rapid and synchronous re-activation of transcription during nc14 and is expressed throughout the mesoderm in only ~10–12 min after mitosis ([Figure S1](#)) [20]. The slow reactivation of *snaE<MS2/yellow* transgenes allowed us to trace the origins of the first nuclei to display post-mitotic reactivation after entry into nc14 ([Figure 1B](#)).

10% to 20% of the pre-mesoderm nuclei (e.g., 26/175) exhibited transcription of the *sna* transgenes by the completion of nc13 ([Figure 1C](#)). After mitosis, five nuclei (~2% of the pattern) exhibited reactivation within 5 min after entry into nc14. Each of these was a descendant of a previously activated mother (“memory mothers”) (see [Movie S1](#) and [Figure S2](#)). During the next several minutes, another 27 nuclei displayed transcription (~9% of the pattern), and over half (15/27) were descendants of memory mothers ([Figure 1C](#), circled in yellow; false-colored in [Movie S1](#)).

During cc13, a small fraction, fr_{13} , of nuclei were active. By the end of cc14, the majority of mesodermal nuclei were active.

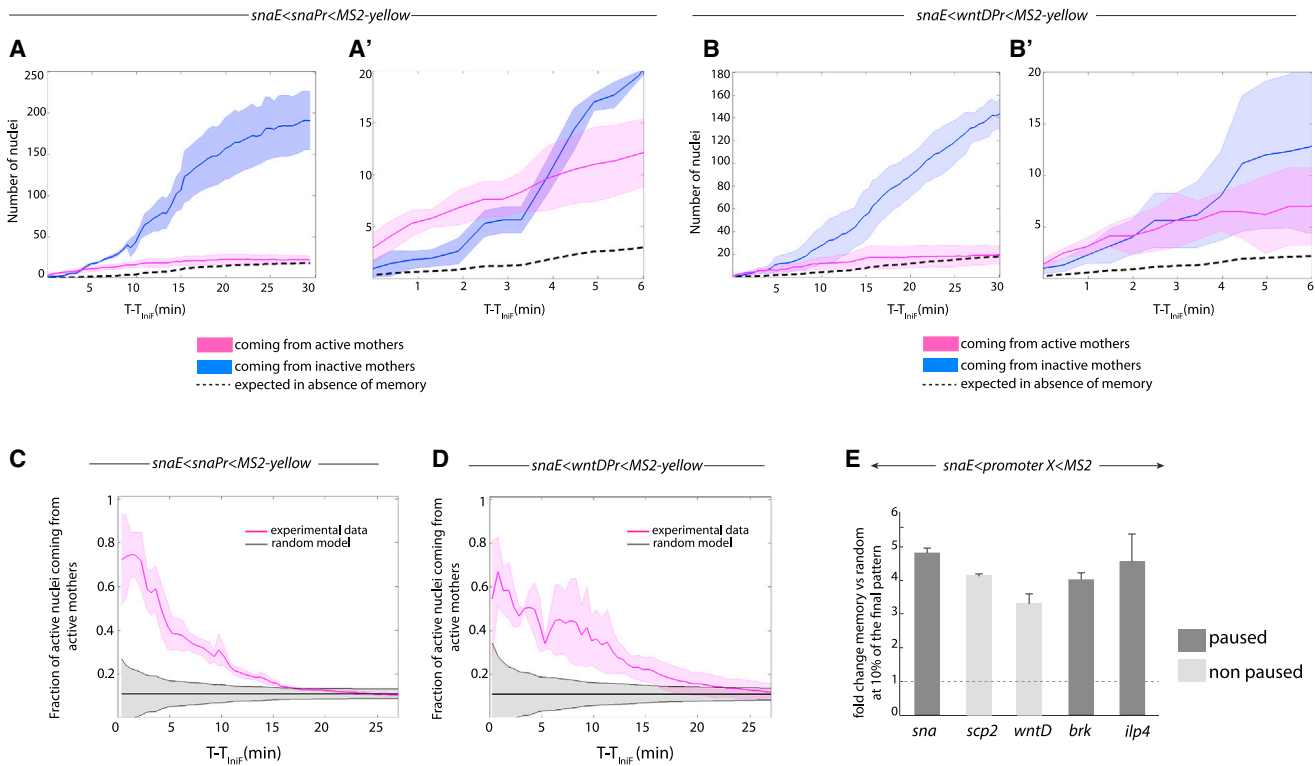


Figure 2. Quantitative Analysis of Transcriptional Memory

(A–B') Memory bias in transcriptional activity during cc14. Kinetics were extracted from three independent movies of *snaE<snaPr<MS2* transgenic embryos (A) and from three independent movies of *snaE<wntDPr<MS2* transgenic embryos (B). The distribution of active nuclei derived from transcriptionally active mother nuclei is shown in pink. The descendants of inactive mother nuclei are depicted in blue. Light colors indicate the SD of these quantified kinetics. Dashed curves represent the expected average time behavior in the absence of a memory bias; for mathematical formulations, please refer to the main text. (A') and (B') show zoomed views of the first 6 min of cc14 corresponding to the plots shown in (A) and (B), respectively.

(C and D) Temporal behavior of the fraction of nuclei derived from memory mothers during cc14 (pink curves). Two different genotypes are shown, with a paused promoter (*snaE<snaPr<MS2*, $n = 3$) (C) or a non-paused promoter (*snaE<wntDPr<MS2*, $n = 3$) (D). Experimental data are compared to the expected behavior of a random activation distribution, indicated in gray, assuming a binomial sampling of a constant fraction of active nuclei in each cell cycle (see the [Supplemental Information](#) for details).

(A–D) For all plots, the x axes correspond to the time (in minutes), starting at the frame where the first spot is detected (TiniF).

(E) Increase in the probability that a memory daughter nucleus is among the first cohort (first 10%) of activated nuclei with respect to the random model expectations during the onset of cc14 for the following transgenes: *snaE<snaPr<MS2* ($n = 3$ movies), *snaE<wntDPr<MS2* ($n = 3$ movies), *snaE<scpPr<MS2* ($n = 2$ movies), *snaE<brkPr<MS2* ($n = 2$ movies), and *snaE<ilp4Pr<MS2* ($n = 2$ movies). The fold change was obtained by division of the fraction of active nuclei coming from active mothers by the fraction expected from the random model. The fold change was evaluated at the time corresponding to 10% of the total active pattern. Error bars represent SEs.

See also [Figure S2](#) and [Movies S2](#) and [S3](#).

The activation of the population of nuclei showed sigmoidal kinetics (see [Figures 2A](#) and [2B](#)). Although a significant fraction of these nuclei were derived from mothers that did not transcribe the transgene during nc13 ([Figure 1C](#), blue circles) (referred to as “non-memory mothers”), quantitative analysis provides clear evidence for memory ([Figure 2](#)). The daughters of memory mothers were approximately four times more likely to be among the first nuclei to display reactivation upon entry into nc14 as compared to a random reactivation ([Movies S1](#) and [S2](#); [Figure 2E](#)). To estimate the temporal dependence of the number of activated nuclei coming from active mothers upon random memoryless activation, we used as a reference the activation kinetics of the nuclei coming from inactive mothers, $N_{14}^{in}(t)$. In the absence of memory, the temporal behavior of active nuclei coming from active mothers, $N_{14}^{act}(t)$, will be the same as that of nuclei coming from inactive mothers,

$N_{14}^{in}(t)$, multiplied by the probability that they do activate fr_{13} : $N_{14}^{act}(t) \sim N_{14}^{in}(t) \cdot fr_{13}$ (shown as dotted lines in [Figures 2A–2B'](#)).

Quantitative analysis of thousands of nuclei in living embryos unequivocally revealed the occurrence of transcriptional memory ([Figure 2](#)). Transgenes containing either the *sna* or *wntD* core promoter exhibited a memory bias ([Figures 2A–2B'](#)). Depending on the promoter sequence, between 60% and 80% of the first cohort of nuclei that were reactivated during the early phases of nc14 derived from memory mothers ([Figures 2C](#) and [2D](#)), which is quite impressive considering that the vast majority of nuclei (~80%–90%) did not express the transgene during nc13 ([Figure 2A](#) and [2B](#)). To test whether the enhanced number of active nuclei coming from active mothers at the beginning of cycle 14 can be explained by stochastic activation alone, we considered a random activation model in which each nucleus

makes an independent decision whether to activate or not. Since all mesodermal nuclei are eventually activated in cc14, the fraction of active nuclei at cc14 coming from active mothers is equal to the fraction fr_{13} of active nuclei at the end of cc13. In the absence of memory, the independent decision of each nucleus to activate or not corresponds to a binomial distribution of activated nuclei with a mean of fr_{13} . The gray shadow in [Figures 2C and 2D](#) shows the random expectation in the absence of memory calculated as the SD of the fraction of activated nuclei coming from active mothers $N_{14}^{act}(t) / N_{14}^{tot}(t)$ as a function of time,

$$SD(t) = \sqrt{\frac{fr_{13} \cdot (1 - fr_{13})}{N_{14}^{tot}(t)}}$$

where $N_{14}^{act}(t)$ is the number of active nuclei coming from active mothers and $N_{14}^{tot}(t)$ is the total number of active nuclei.

Despite the relatively small number of nuclei constituting the first cohort of activation, the observed distribution was non-random ([Figures 2C and 2D](#)). The proportion of memory nuclei exhibiting reactivation progressively diminished to 30%, 20%, and 10% during the next 5, 10, and 15 min, respectively ([Figures 2C and 2D](#)).

These observations leave little doubt that transcription of *sna* transgenes during nc13 predisposes them for rapid reactivation during nc14 as compared with inactive nuclei. In fact, transcription during nc13 resulted in a 3.5-fold to 5-fold increase in the likelihood of daughter nuclei exhibiting reactivation during the initial phases of nc14 ([Figures 2E and S3A–S3D](#)). The efficiency of this transcriptional memory was influenced by the different promoter sequences tested in this study. The *sna* and *ilp4* promoters yielded a higher efficiency of reactivation during the initial phases of nc14 than does the *wntD* promoter. The basis for these differences is uncertain, but they do not scale with the levels of paused Pol II identified by tissue-specific embryonic Pol II chromatin immunoprecipitation or global run-on sequencing assays [11, 21]. Moreover, memory was observed regardless of the presence (e.g., *sna* promoter) or absence (e.g., *brk* promoter) of the TATA box sequence, despite previous reports that TBP remains bound to mitotic chromosomes and fosters post-mitotic re-activation [22]. The *brk* promoter is not bound by TBP in the pre-cellular embryo [23], even though our movies clearly demonstrate a memory bias in the reactivation of the *snaE<brk<MS2* transgene. Thus, other mechanisms of mitotic “bookmarking” might be at play (see below).

At least two mechanisms can be envisioned for transcriptional memory, asymmetric distribution of activators and inheritance of transcribed templates. *Sna* is activated by Dorsal and Twist, which are distributed in gradients. In principle, there could be slight variations in their distributions even among nuclei located in ventral regions where there are peak concentrations of both activators. Perhaps a few “jackpot” nuclei obtain higher levels of Dorsal and Twist, which are subsequently inherited by daughter nuclei. Alternatively, transcription of a DNA template might render it more susceptible to rapid reactivation after mitosis. Transcription could cause inherited changes in the distribution of DNA-bound transcription factors, nucleosomes, or histone modifications favoring activation in the next cell cycle.

In an effort to distinguish between these alternative models, we quantified the inheritance patterns of neighboring active and inactive mother nuclei during the transition from nc13 to nc14 ([Figures 3A, 3B, 3F, 3G, and S3G–S3J](#)). Most active mother nuclei produced just one daughter nucleus that rapidly reactivates the *sna* transgene during the early phases of nc14. The activation time for memory daughters was approximately two times faster than that for descendants of a neighboring non-active mother ([Figure 3B](#)). The second “memory daughter” displayed expression only after a delay (8.5 ± 6.2 min); however, the activation of this second memory daughter is significantly faster than that of the second non-memory daughter ([Figure 3C](#)). To explain these observations, we hypothesize that, in most cases, only one of the two sister chromatids of the homolog containing the transgene initiates transcription detected by the MS2-MCP technique (summarized in [Figure S2C](#)).

Many genes are duplicated on tightly associated sister chromatids during the late S and G2 phases of cc14 [24]. Among others, one possible interpretation of these inheritance patterns is that the *sna* transgene is transcribed by only one of the two sister chromatids during nc13 ([Figure S2](#)).

The inheritance patterns observed for homozygotes carrying two copies of the transgene are consistent with this interpretation ([Movie S3](#)). Mother nuclei exhibiting transcription of both copies of the transgene during nc13 display two different inheritance patterns at roughly equal frequencies. Some produce two daughters that each contains a single transcription dot at the onset of nc14 (1,1 configuration). Others produce one daughter with two dots and a sister that lacks early reactivation signals (2,0 configuration) ([Figures S2B and S2D](#)). A simple interpretation of these observations is the independent assortment of active and inactive sister chromatids during mitosis (summarized in [Figure S2D](#)).

These observations could be explained by an allelic specific inheritance of memory, but also by an unequal distribution of transcriptional activators between two daughters. However, if one “jackpot” descendant inherited higher amounts of activators, this would increase the probability of activation of the MS2 transgene and cause frequent asymmetric inheritance configurations, namely (1,0) or (2,0). Manual analysis of three independent *snaE<snaPr<MS2* homozygous movies disfavors such asymmetric inheritance patterns ([Movie S3; Figure S2](#)). Moreover, unequal distribution of activators seems unlikely in syncytial embryos, where there is extensive intermingling of nuclei during mitosis (see [Movies S1, S2, and S3](#)). Our analysis was restricted to the ventral-most regions, where there are peak levels of the Dorsal and Twist activators. We have not included nuclei located in ventro-lateral regions, where there are diminishing levels of activator gradients. Indeed, measurement of the activation time of nuclei as a function of the distance to the ventral furrow dismisses the existence of a spatial bias responsible for transcriptional memory ([Figures 3F, 3G, and S3G–S3J](#)).

The basis for transcriptional memory is uncertain. It can be as simple as the displacement of nucleosomes at the core promoter [25], thereby facilitating the recruitment of Pol II upon entry into nc14. Alternatively, active transcription during nc13 might lead to certain histone modifications at the enhancer and/or promoter (e.g., H4K5ac or H3K4me) that are retained during mitosis and

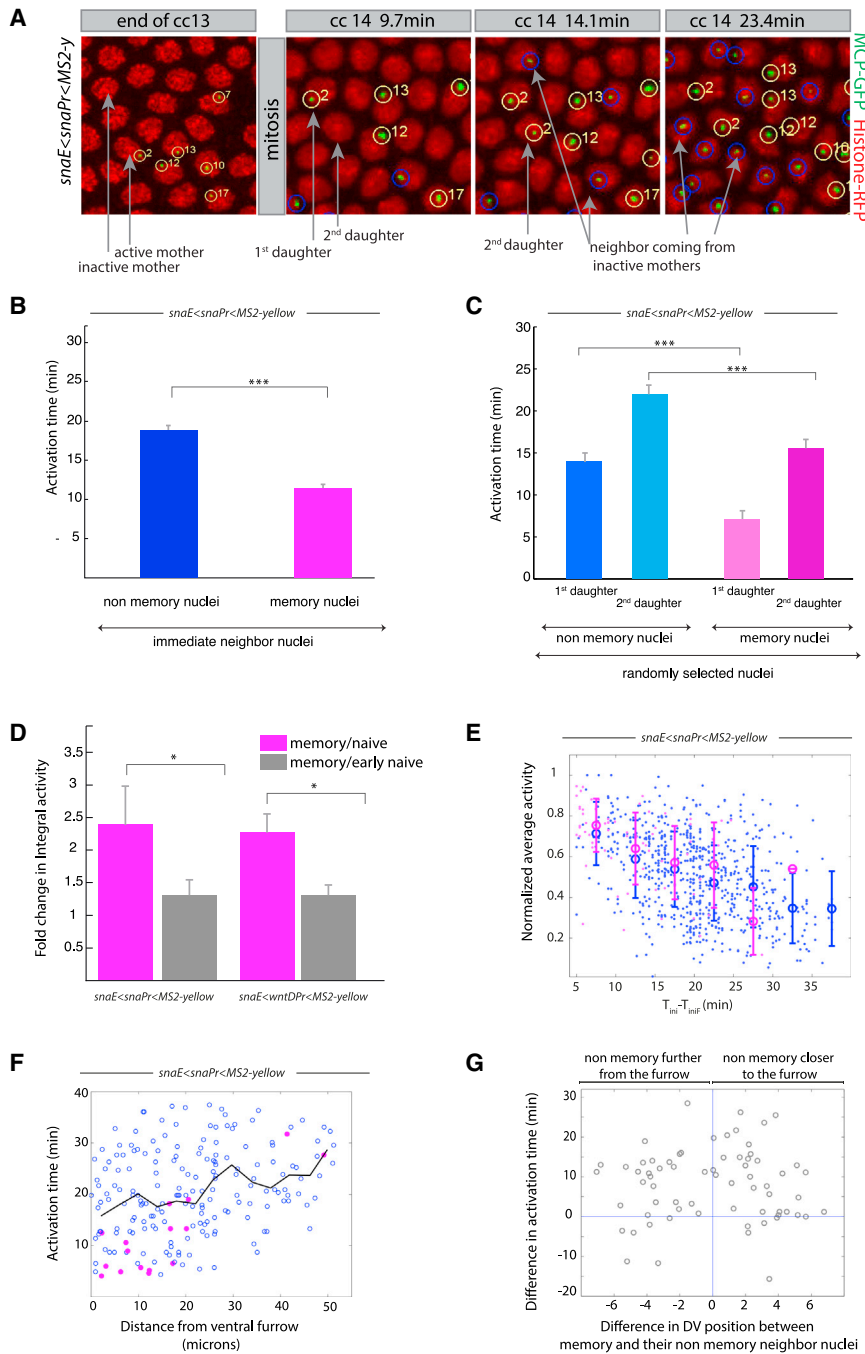


Figure 3. Transcriptional Kinetics of Memory

(A) Snapshots of live imaging of a *snaE<snaPr<MS2* transgenic embryo. Confocal z-projected images of selected ventral regions are shown at different time points during cc13 and cc14. Tracked active nuclei at cc13 and their descendants (first and second daughter to exhibit transcription) are circled and numbered in yellow. Examples of immediate neighboring nuclei coming from inactive mother nuclei are circled in blue.

(B) Mean activation time for descendants of active mother nuclei and for immediate neighboring nuclei coming from inactive mothers. Error bars represent SEs (non-memory nuclei are shown in blue, $n = 68$; memory nuclei are shown in pink, $n = 68$; memory versus non-memory, $p = 3 \times 10^{-10}$).

(C) Mean activation time for descendants of active mother nuclei or those from inactive mothers, tracking the first daughter and second daughter separately, randomly selected from the entire imaged region. Error bars represent SEs (first daughter non-memory, $n = 54$; second daughter non-memory, $n = 54$; first daughter memory, $n = 24$; second daughter non-memory $n = 24$; first daughter non-memory versus first daughter memory, $p = 3 \times 10^{-8}$; second daughter non-memory versus second daughter memory, $p = 1 \times 10^{-4}$).

(B and C) Quantification was performed on three movies of *snaE<snaPr<MS2* transgenic embryos (total of 750 nuclei).

(D) Fold change in integral activity, defined as the ratio between the integral activity of memory nuclei divided by that of non-memory nuclei. Integral activity corresponds to the sum of activities across all time frames. Error bars represent SEs computed on three different movies for each genotype (*snaE<snaPr<MS2*, $p = 0.02$; *snaE<wntDPr<MS2*, $p = 0.03$).

(E) This scatterplot shows the behavior of the average activity as a function of the activation time. The data points were extracted from three movies, and the value of the average activity was normalized by its maximum. Nuclei coming from active mothers are depicted in pink, and those coming from inactive mothers are depicted in blue. Error bars are SDs evaluated by binning of the activation time in intervals of 5 min each.

(F) Scatterplot of the activation time as function of the distance from the ventral furrow at cc14 for a *snaE<snaPr<MS2* transgenic embryo. Pink symbols represent memory nuclei, and blue symbols non-memory ones. The black line indicates the average behavior.

(G) Scatterplot of the difference in activation time between a memory nucleus and its non-memory closest neighbor as function of their distance. The statistical test used was a two-sample t test with the following convention: $*0.05 < p < 0.01$, $**0.01 < p < 0.001$, $***p \leq 0.001$. See also [Figure S3](#) and [Movies S2](#) and [S3](#).

foster rapid reactivation in the ensuing cell cycle, as observed in cultured cells [3], *Dictyostelium* [2], and yeast [26].

In the early *Drosophila* embryo, genome-wide H3K4methylation (H3K4me3 or H3K4me1) is detected at the maternal-zygotic transition [23, 27], occurring at the transition between nc13 and nc14, precisely when we observe transcriptional memory. It is therefore possible that histone methylation, established during

zygotic genome activation, provides the basis for transcriptional memory.

Is transcriptional memory used to help pattern the *Drosophila* embryo? To address this question, we investigated the levels of transcription produced from nuclei derived from active and inactive mothers. The goal was to determine whether memory nuclei exhibit more efficient expression of the *sna* transgene

than non-memory nuclei during nc14. According to such a scenario, transcription might be progressive, leading to increasing efficiencies in the production of mRNAs due to prior “priming” events. Rates of RNA synthesis can be extrapolated by measuring the average fluorescence intensities (MS2-MCP-GFP) at the transcription foci [6, 7].

Average fluorescence intensities were inversely correlated with the delay in gene re-activation (Figures 3D, 3E, S3E, and S3F). The earlier a nucleus is activated, the higher its time-averaged rate of RNA synthesis (Figures 3D and 3E). Consequently, memory nuclei produced during nc14, on average, ~2-fold more mRNAs than non-memory nuclei (Figure 3D). Moreover, there was a reduction in the levels of RNAs produced by late-expressing nuclei (mainly non-memory daughters) (Figures 3E and S3F) due to an overall reduction in the levels of *sna* expression during nc14 [28].

In summary, we propose that transcriptional memory contributes to the rapid and synchronous activation of gene expression seen in the early *Drosophila* embryo. Memory might also be important for the sustained expression of constitutive “house-keeping” genes during successive cell cycles. Indeed, transcriptional memory has been documented for the *actin5* gene in *Dictyostelium* [2]. Finally, we suggest that transcriptional memory is a mechanism of developmental homeostasis, which helps ensure, when needed, that cells will tend to retain the properties of their progenitors. However, this transcriptional persistence could in principle impede the plasticity required during cell specification.

EXPERIMENTAL PROCEDURES

All MS2 containing transgenic embryos were generated by the targeted integration (VK33) of *snaEnhancer*<minimal promoter>24X-MS2 repeats-yellow plasmids [10]. Histone-RFP and MCP-GFP were maternally provided by a stock described in [6]. All movies were acquired using a Zeiss LSM780 confocal microscope with the following settings: a 40× oil objective and a 2.1 zoomed 512 × 512 16 bit/pixel image, with bidirectional scanning and 21 z stacks 0.5 μm apart. Under these conditions, the time resolution is in the range of 15–20 s per frame. Image processing of the MS2-MCP-GFP signal was performed in a semi-automatic way using custom MATLAB algorithms, based on our previously published work [5]. See the [Supplemental Experimental Procedures](#) for details on transgenic fly stocks, molecular biology, imaging, and quantification. All animal usage was under the approval of the University of Berkeley California Institutional Animal Care and Use Committee.

SUPPLEMENTAL INFORMATION

Supplemental Information includes Supplemental Experimental Procedures, three figures, and three movies and can be found with this article online at <http://dx.doi.org/10.1016/j.cub.2015.11.058>.

ACKNOWLEDGMENTS

We are grateful to Thomas Gregor and Hernan Garcia for sharing the MCP-GFP fly stock. We would like to thank Wei Zhang for his help with genomic data analysis. M. Lagha was a recipient of a HFSP long-term fellowship and is currently sponsored by the CNRS. T.F., N.D., A.M.W., and M.C. are supported by grant nos. ANR AXOMORPH, ANR-11-LABX-0044, and ANR-10-IDEX-0001-02PSL. T.F. and A.M.W. are supported by MCCIG grant no. 303561. This research was initiated in the M. Levine lab with a support from NIH grant RO1 GM34431. The M. Lagha lab is supported by an ATIPE-Avenir CNRS grant and an HFSP CDA grant.

Received: June 29, 2015

Revised: October 5, 2015

Accepted: November 12, 2015

Published: December 31, 2015

REFERENCES

1. Porcher, A., Abu-Arish, A., Huart, S., Roelens, B., Fradin, C., and Dostatni, N. (2010). The time to measure positional information: maternal hunchback is required for the synchrony of the Bicoid transcriptional response at the onset of zygotic transcription. *Development* 137, 2795–2804.
2. Muramoto, T., Müller, I., Thomas, G., Melvin, A., and Chubb, J.R. (2010). Methylation of H3K4 is required for inheritance of active transcriptional states. *Curr. Biol.* 20, 397–406.
3. Zhao, R., Nakamura, T., Fu, Y., Lazar, Z., and Spector, D.L. (2011). Gene bookmarking accelerates the kinetics of post-mitotic transcriptional re-activation. *Nat. Cell Biol.* 13, 1295–1304.
4. Sigal, A., Milo, R., Cohen, A., Geva-Zatorsky, N., Klein, Y., Liron, Y., Rosenfeld, N., Danon, T., Perzov, N., and Alon, U. (2006). Variability and memory of protein levels in human cells. *Nature* 444, 643–646.
5. Lagha, M., Bothma, J.P., and Levine, M. (2012). Mechanisms of transcriptional precision in animal development. *Trends Genet.* 28, 409–416.
6. Lucas, T., Ferraro, T., Roelens, B., De Las Heras Chanes, J., Walczak, A.M., Coppey, M., and Dostatni, N. (2013). Live imaging of bicoid-dependent transcription in *Drosophila* embryos. *Curr. Biol.* 23, 2135–2139.
7. Garcia, H.G., Tikhonov, M., Lin, A., and Gregor, T. (2013). Quantitative imaging of transcription in living *Drosophila* embryos links polymerase activity to patterning. *Curr. Biol.* 23, 2140–2145.
8. Lamouille, S., Xu, J., and Derynck, R. (2014). Molecular mechanisms of epithelial-mesenchymal transition. *Nat. Rev. Mol. Cell Biol.* 15, 178–196.
9. Hemavathy, K., Meng, X., and Ip, Y.T. (1997). Differential regulation of gastrulation and neuroectodermal gene expression by Snail in the *Drosophila* embryo. *Development* 124, 3683–3691.
10. Ip, Y.T., Park, R.E., Kosman, D., Yazdanbakhsh, K., and Levine, M. (1992). Dorsal-twist interactions establish snail expression in the presumptive mesoderm of the *Drosophila* embryo. *Genes Dev.* 6, 1518–1530.
11. Lagha, M., Bothma, J.P., Esposito, E., Ng, S., Stefanik, L., Tsui, C., Johnston, J., Chen, K., Gilmour, D.S., Zeitlinger, J., and Levine, M.S. (2013). Paused Pol II coordinates tissue morphogenesis in the *Drosophila* embryo. *Cell* 153, 976–987.
12. Perry, M.W., Boettiger, A.N., Bothma, J.P., and Levine, M. (2010). Shadow enhancers foster robustness of *Drosophila* gastrulation. *Curr. Biol.* 20, 1562–1567.
13. Dunipace, L., Ozdemir, A., and Stathopoulos, A. (2011). Complex interactions between cis-regulatory modules in native conformation are critical for *Drosophila* snail expression. *Development* 138, 4075–4084.
14. Harrison, M.M., Li, X.-Y., Kaplan, T., Botchan, M.R., and Eisen, M.B. (2011). Zelda binding in the early *Drosophila melanogaster* embryo marks regions subsequently activated at the maternal-to-zygotic transition. *PLoS Genet.* 7, e1002266.
15. Nien, C.-Y., Liang, H.-L., Butcher, S., Sun, Y., Fu, S., Gocha, T., Kirov, N., Manak, J.R., and Rushlow, C. (2011). Temporal coordination of gene networks by Zelda in the early *Drosophila* embryo. *PLoS Genet.* 7, e1002339.
16. Foo, S.M., Sun, Y., Lim, B., Ziukaite, R., O'Brien, K., Nien, C.-Y., Kirov, N., Shvartsman, S.Y., and Rushlow, C.A. (2014). Zelda potentiates morphogen activity by increasing chromatin accessibility. *Curr. Biol.* 24, 1341–1346.
17. Szymanski, P., and Levine, M. (1995). Multiple modes of dorsal-bHLH transcriptional synergy in the *Drosophila* embryo. *EMBO J.* 14, 2229–2238.
18. Groth, A.C., Fish, M., Nusse, R., and Calos, M.P. (2004). Construction of transgenic *Drosophila* by using the site-specific integrase from phage ϕ C31. *Genetics* 166, 1775–1782.

19. Zeitlinger, J., Stark, A., Kellis, M., Hong, J.-W., Nechaev, S., Adelman, K., Levine, M., and Young, R.A. (2007). RNA polymerase stalling at developmental control genes in the *Drosophila melanogaster* embryo. *Nat. Genet.* *39*, 1512–1516.
20. Bothma, J.P., Garcia, H.G., Ng, S., Perry, M.W., Gregor, T., and Levine, M. (2015). Enhancer additivity and non-additivity are determined by enhancer strength in the *Drosophila* embryo. *eLife* *4*, e07956.
21. Saunders, A., Core, L.J., Sutcliffe, C., Lis, J.T., and Ashe, H.L. (2013). Extensive polymerase pausing during *Drosophila* axis patterning enables high-level and pliable transcription. *Genes Dev.* *27*, 1146–1158.
22. Xing, H., Vanderford, N.L., and Sarge, K.D. (2008). The TBP-PP2A mitotic complex bookmarks genes by preventing condensin action. *Nat. Cell Biol.* *10*, 1318–1323.
23. Chen, K., Johnston, J., Shao, W., Meier, S., Staber, C., and Zeitlinger, J. (2013). Author response. *eLife* *2*, e00861.
24. McKnight, S.L., and Miller, O.L., Jr. (1979). Post-replicative nonribosomal transcription units in *D. melanogaster* embryos. *Cell* *17*, 551–563.
25. Lenhard, B., Sandelin, A., and Carninci, P. (2012). Metazoan promoters: emerging characteristics and insights into transcriptional regulation. *Nat. Rev. Genet.* *13*, 233–245.
26. Brickner, J.H. (2009). Transcriptional memory at the nuclear periphery. *Curr. Opin. Cell Biol.* *21*, 127–133.
27. Li, X.-Y., Harrison, M.M., Villalta, J.E., Kaplan, T., and Eisen, M.B. (2014). Establishment of regions of genomic activity during the *Drosophila* maternal to zygotic transition. *eLife* *3*, e03737.
28. Boettiger, A.N., and Levine, M. (2013). Rapid transcription fosters coordinate snail expression in the *Drosophila* embryo. *Cell Rep.* *3*, 8–15.